Journal of Zhejiang University-SCIENCE A (Applied Physics & Engineering)
ISSN 1673-565X (Print); ISSN 1862-1775 (Online)
www.zju.edu.cn/jzus; www.springerlink.com
E-mail: jzus@zju.edu.cn

An approach to the capsule endoscopic robot with active drive motion*

Da-qiang GU†, Yong ZHOU
(*Department of Mechanical Engineering, Zhejiang University, Hangzhou 310027, China*)
†Email: gudq@zju.edu.cn

Received Apr. 6, 2010; Revision accepted July 23, 2010; Crosschecked Jan. 25, 2011

Abstract: Commercialized capsule-type endoscopes move passively by peristaltic waves (and gravity), which makes it difficult for doctors to diagnose the areas of interest more thoroughly and actively. To resolve this problem of passivity, it is necessary to find a special locomotion principle, which fits the gastrointestinal (GI) tract. In this paper, a legged locomotive mechanism with shape memory alloy (SMA) actuation based on the peristaltic principle is proposed, and then the structure of the locomotion mechanism is introduced. Based on the preliminary results, the design, modeling, and fabrication of an SMA microactuation concept for application in an endoscopic capsule are given, as well as the SMA spring and legged component design, which is the core section of the system design. We used the pseudo-rigid-body model (PRBM) to analyze nonlinear and large deflections of the SMA legged component. Thus, a prototype endoscope with an SMA spring and six legged components was designed and fabricated. It is 15 mm in diameter and 33 mm in total length, with a hollow space to house other parts needed for endoscopy such as a camera, a radio frequency (RF) module, and sensors. During testing, the locomotive mechanism was effective in a plastic tube environment.

Key words: Capsular endoscopy, Shape memory alloy (SMA), Microactuation, Locomotion
doi:10.1631/jzus.A1000141 **Document code:** A **CLC number:** TH77

1 Introduction

An endoscope is used to diagnose various diseases throughout the gastrointestinal (GI) tract. The GI tract is a 30 foot long structure, which includes the esophagus, stomach, intestine, and colon. It is difficult for the long traditional endoscope to reach some parts of the digestive tract where are narrow and convoluted, and some blind spots. Traditional endoscopy tools have a somewhat high stiffness, and it may be uncomfortable or painful for patients when the doctor inserts and rotates the tools (Appleyard *et al*., 2000; Kim *et al*., 2005a).

These problems led to the development of wireless capsule endoscopes. The capsule endoscopy system is composed of several key parts, the capsule itself, a portable image receiver/recorder unit and battery pack, and a specially modified computer workstation. The capsule endoscope is a miniature capsule, which is used to record pictures through the digestive tract (Fig. 1). The capsule contains an imaging system, often a camera, with the shape and size of a pill, used to visualize the GI tract. Due to the development of wireless capsule endoscopes, it is now possible to diagnose small intestinal lesion, which cannot readily be achieved by traditional endoscopes, and also to reduce discomfort and pain for patients.

The first capsule endoscope named M2A was developed and commercialized in 2001 by Given Imaging Inc. of Israel. It is 10 mm in diameter and

---

[*] Project (No. 50375143) supported by the National Natural Science Foundation of China

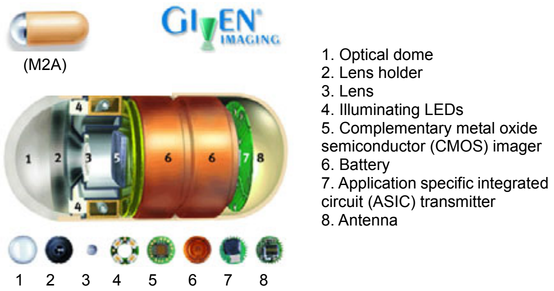

Fig. 1 Capsule endoscope

27 mm long, with illuminating LEDs, a complementary metal oxide semiconductor (CMOS) camera, a radio frequency (RF) module, and a battery integrated. M2A was approved by the US Food and Drug Administration (FDA) in August 2001. It can be swallowed, and transmit wireless still and moving pictures from the GI tract. Another wireless capsule endoscope called Noika V3 was developed by RF System Co. Ltd. in Japan (Moglia *et al.*, 2007). At the present time, the capsule endoscope is primarily used to visualize the entire small intestine, being ideally suited for searching obscure or occult GI bleeding in patients, who have undergone an inconclusive standard evaluation.

However, capsule endoscopes only have an approximate fifty percent success rate for detecting diseased areas. This low percentage is due to the lack of direct and effective control over its position, orientation, and speed (Cheung *et al.*, 2005). Those microcapsules move passively by the natural peristaltic motion of the digestive tract, and thus, they can only move ahead without the ability to turn, stop, or go back during the journey inside the GI tract. The microcapsules cannot be controlled by the doctors to observe, detect, and analyze pathological areas of interest, or to accomplish medical tasks like biopsy and drug delivery.

A tele-operated capsule endoscope provided with an active locomotion system would solve these problems. However, as the GI tract has the natural characteristics of being slippery, convoluted, soft, villous, and elastic, typical robotics mechanisms are inefficient and likely to fail. To date, no practical solutions for active locomotion in the GI tract have been developed, and a locomotion model in such a slippery and deformable environment is still largely unexplored (Menciassi *et al.*, 2004).

Our objective is to provide an autonomous locomotion mechanism, which could be integrated into an endoscopic robot that can propel itself in the human GI tract.

2 Locomotion principle

While the endoscopic microcapsule works inside the human body, it should contain a camera module, RF module, battery module, etc, and its design is different from other robots. Due to the complex operating environment and size constraints, the main features required for the design of an endoscopic capsule are as follows:

1. Space requirement. As the robot moves in the GI tract, the overall size of the robot is limited, and we must leave a certain space for the power module, vision module, telemetry module, actuation module, and central processing module, etc. Thus, the number of transmission chains of the drive system should be minimized to integrate other modules.
2. Practical requirement. As the capsule robot is swallowed from the mouth, and will eventually be excreted from the anus with waste, we need consider the external shape of the capsule robot to make it swallowable and painless.
3. Biocompatible and safe requirement. As the endoscopic robot moves in the human body, it must be made of safe and non-toxic materials, and the external materials must be biocompatible.
4. Corrosion resistant requirement. As intestinal mucus is present, the endoscopic robot should be able to resist the intestinal mucus.

Taking into account the above points, many traditional actuators are not suitable for the proposed application. Many research institutions in the world are devoting considerable efforts to developing active locomotion systems to be incorporated into wireless endoscopic capsules, and to designing various endoscopic robots with different drive mechanisms. Sendoh *et al.* (2003) proposed a locomotive system applying a magnetic actuator composed of a magnet and a spiral structure to a capsule endoscope. The actuator was rotated and propelled wirelessly by applying an external rotational magnetic field. Kim *et al.* (2005b) designed an earthworm-like locomotive mechanism for capsule endoscopes integrated with an impact based piezo actuator and engraved clampers.

Park *et al.* (2007) proposed a new paddling based locomotive mechanism for endoscopic capsules. Quirini *et al.* (2007) developed a motor based legged capsule. Li *et al.* (2006) proposed a locomotion principle, which is obtained by simulating, analyzing, and simplifying the movement of mucus-cilia system. Zabulis *et al.* (2008) explored the vibratory actuation employing eccentric-mass micromotors on endoscopic capsule. Moon *et al.* (2007) presented an electrical stimuli capsule using the designed RF system. Zhou *et al.* (2001) designed a spiral-type non-invasive endoscopic microrobot driven by the towing force caused by two running spirally grooved cylinders.

According to environmental characteristics of the intestine, in this study, combined with the characteristics of creeping robots and legged robots, a kind of legged robot with the peristaltic principle is designed. As the intestine is a cylindrical-shape structure, the designed microrobot has two groups of legged devices, and each group is axisymmetrically distributed on the main robot body.

With the microcontroller, we can control the robot's motion and precise position by identifying the gait pattern. As the microrobot moves in human intestinal tract, considering the effect of gravity and intestinal peristalsis, the robot's forward movement is different with backward movement. The working principles of the backward and forward movements of microrobot are shown in Fig. 2. A cycle of the reverse movement in the intestine can be divided into nine gaits:

Gait 1: at the beginning, the robot is in the initial stage.

Gait 2: the linear spring component stretches.

Gait 3: the fore leg-shaped components open to center the robot inside the GI lumen and to firmly hook it on the tissue.

Gait 4: the linear spring component contracts.

Gait 5: the hind leg-shaped components open to make the robot stay on the intestine wall.

Gait 6: the fore leg-shaped components close to return to the original state.

Gait 7: the linear spring component opens, and the robot moves one step backward.

Gait 8: the hind leg-shaped components close to return to the original state.

Gait 9: the linear spring component contracts and returns to its original state.

After one cycle, the robot moves one step forward. Moving in this cycle, the endoscopic microrobot can realize forward movement in the intestine.

Due to the effect of gravity and intestinal peristalsis, the controllable upright movement of the microrobot in the small intestine does not simply reverse the order of inverse controlled motion. As shown in Fig. 2b, a cycle of the upright movement can be divided into six gaits:

Gait 1: at first, the robot is in the initial stage.

Gait 2: the spring component stretches.

Gait 3: the fore leg-shaped components open to center the robot inside the GI lumen and to firmly hook it on the tissue.

Gait 4: the linear spring component contracts.

Gait 5: the intestinal peristaltic force pushes the robot's main body to move one step forward.

Gait 6: the fore leg-shaped components close to return to the original state.

The endoscopic robot can be controlled to move forward and reversely in the human small intestine by a single-chip microcomputer (SCM).

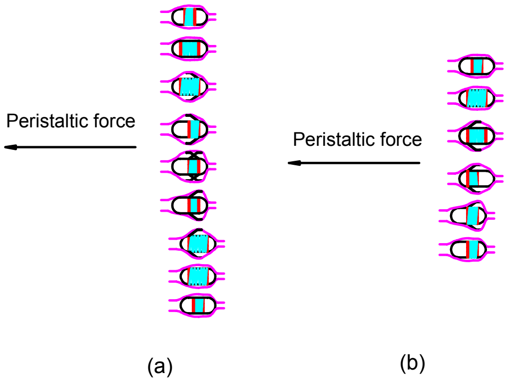

Fig. 2 Locomotion gait sequence
(a) Backward movement; (b) Forward movement

3 Structure design of the endoscopic robot

3.1 Choice of drive materials

In the design of the drive mechanism of the endoscopic robot, we have to consider the design requirements in terms of the size, power, force, motion range, and safety. Considering these requirements, many conventional actuators are not suitable for the proposed locomotion principle. For example, piezoelectric actuators have fast response time, and could produce very large output forces. However, they require a complex electro-circuit to supply a high input voltage, and they have a very short stroke, which needs mechanical amplification systems to generate usable displacements, which in turn could increase the total size of the robot. Electro-active polymer (EAP) actuators could have large resilience and good bio-applicability, but respond very slowly, and consume a large amount of energy. Furthermore, they cannot produce large forces. Micro brushless direct current (DC) motor actuators should provide very high output torque, but they need to turn rotation into a linear movement through transmission, with a large output power, and the size is too large to integrate other modules.

Based on the above considerations, shape memory alloy (SMA) actuators seem to be the best solution for developing the prototypal actuation system of the legged endoscopic robot. This choice has been preferred for the following interesting features of SMA actuators (Gorini *et al*., 2006):

1. They are characterized by high output forces with high displacements.
2. SMAs have a high power to weight ratio (up to ten times that of traditional actuation systems). Thus, it is possible to realize a very compact actuation system that may be matched with the capsules body dimension.
3. They have good biocompatibility.

Unfortunately, SMAs also have some drawbacks like low bandwidth (3 Hz), high power consumption, bad controllability, and slow response speeds. Despite these negative aspects, SMA actuators have been selected for the possibility of realizing a compact actuation system and achieving an easily integration into the capsule (Kim *et al*., 2004).

In the design, a two-way SMA is used for the size consideration. It can remember two different shapes: one at low temperatures and the other a high temperature shape.

3.2 Program design

For the integration of other modules of the capsule endoscope, the inside of the capsule robot leaves a certain space, two groups of legged mechanism are placed on the lateral surface of the microrobot, and each group has three sets of legged devices, which ensure the microrobot to fully contact the intestinal wall. The legged structures are fixed on a circular ring structure, and the circular ring structure can slide inside the capsule robot. The legged mechanism can shrink inside the capsule robot, so it will not cause harm to the human body when swallowed and discharged.

Fig. 3 shows the modeling structure of the capsule robot. The main body is 15 mm in diameter, and 33 mm in length; and the legged structure is 18 mm in length, 1.6 mm in width, and 0.3 mm in height.

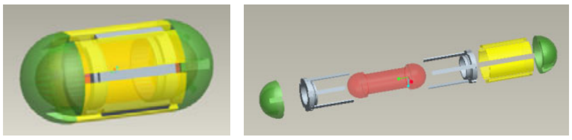

Fig. 3 Model of the capsule robot

3.3 Legged shape memory alloy (SMA) structure

The SMA actuator system normally includes SMA-drive and execution components. However, due to the size restriction of the capsule endoscopy, we consider taking the SMA-drive component as an execution component to facilitate the integration of other modules. Therefore, the robot's legged components are made of SMA directly. Loctite 495 is used to fix the legged structure on the ring structure. One end (0–2 mm) of the legged structure will maintain a straight linear structure at low and high temperatures, while the other end will be bent round at high temperatures (Fig. 4), and the bent end's deformation would reach 7 mm in the vertical direction.

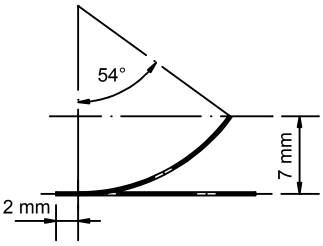

Fig. 4 Legged shape memory alloy (SMA) structure

3.4 Ring structure

The ring structure is used to the fix the legged structures and spring structure. One end of the ring structure has a screw structure to fix the spring structure (Fig. 5). There are six grooves at the outside surface to fix the legged structures and to facilitate movement of the legged structures. As the ring structure needs to directly contact SMA components, it is made of photosensitive resin, which is insulating and high temperature resistant, and the circular structure can slide inside the capsule robot.

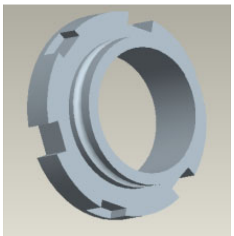

Fig. 5 Ring structure of the robot

3.5 Design and manufacture of other major components of the microrobot

The robot's main body and some auxiliary connecting mechanisms are fabricated of photosensitive resin by stereolithography apparatus (SLA) rapid prototyping. Stereolithography is a rapid prototyping process utilizing a 3D CAD model to produce a physical object. It creates prototypes layer by layer based on physical layer manufacturing principles. DSM Somos 14120 resin is selected to manufacture those parts. The resin is a low viscosity liquid photosensitive polymer, which produces tough, strong, and water resistant parts. Products created with the resin have a white and opaque appearance similar to production plastics.

Some products made of photosensitive resin are shown in Fig. 6. The accuracy of the manufacturing model made by SLA rapid prototyping technology can reach 0.1 mm, and the products have a smooth surface.

Fig. 6 Prototype of some parts of the robot

4 Parameters design of key components

4.1 Mechanical model of the endoscopic robot

Fig. 7 shows the mechanical model of the microrobot in the small intestine. Contraction of longitudinal muscle and circular muscle together push the robot forward with the diameter of one end of the small intestine in a smaller state. Both ends are of hemispherical shapes. Some conclusions are described in detail as follows:

$$F_r=G\sin\theta+Z+T, \tag{1}$$

$$3F_x>F_s>F_r, \tag{2}$$

where G is the gravity of the capsule robot, Z is the intestinal peristaltic force, T is the viscous resistance of the intestinal mucus, F_r means the resistance of the microrobot moving in the intestine, F_s is the restoring force of the SMA spring, and F_x and F_y mean the component forces between the intestine and the legged SMA structure.

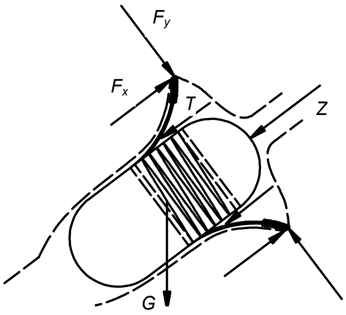

Fig. 7 Mechanical model of the microrobot

4.2 Design of the shape memory alloy (SMA) spring

As the characteristics of the SMA spring are closely related to temperature, its performance is different from an ordinary spring. The difference is mainly manifested as follows (Yang and Wu, 1993):

1. For an ordinary spring, the relationship between stress and strain is linear, while it is nonlinear for the SMA spring. Take Ti-Ni SMA for example, the value of elastic modulus varies by 300% from parent phase to martensite phase.

2. The properties of an ordinary spring basically have nothing to do with the temperature, while the characteristics of the SMA spring are closely related to temperature.

3. The characteristic strain-stress curves basically coincide in the process of loading and unloading for an ordinary spring, while the characteristic curves of the SMA spring are mostly not overlapped. There is a temperature hysteresis or strain hysteresis phenomenon. Thus, the design formulas of a normal spring cannot be simply used.

The maximum shear stress of a linear elastic spring is

$$\tau = W\frac{8PD}{\pi d^3}, \tag{3}$$

where P is the external axial force, D means the spring coil diameter, and d is the diameter of the spring wire (Rogers, 1997). W is the Wahl correction factor, and is given as

$$W = \frac{4C-1}{4C-4} + \frac{0.615}{C}, \tag{4}$$

where C means the spring curvature.

Then the shear strain ξ can be calculated by

$$\xi = \frac{J}{\tau}. \tag{5}$$

The relationship of the shear modulus and elastic modulus is as follows:

$$J_{\mathrm{a}} = \frac{E_{\mathrm{a}}}{2(1+\upsilon)}, \tag{6}$$

$$J_{\mathrm{m}} = \frac{E_{\mathrm{m}}}{2(1+\upsilon)}, \tag{7}$$

where J is the material shear modulus, E is Young's modulus, and υ is Poisson's ratio. The subscripts 'a' and 'm' indicate the corresponding spring is heated and cooled, respectively.

The total number of active coils can be calculated by

$$n = \frac{\delta d}{\pi \xi D^2}, \tag{8}$$

where δ is the deformation of the spring in high temperatures.

According to the size requirements of the capsule model, let D=9.5 mm, d=1 mm, δ=3 mm, and n=9.

4.3 Design of legged shape memory alloy (SMA) components

As the legged SMA components have large, nonlinear deflection, the traditional methods of deflection analysis do not apply. This can be solved using the pseudo-rigid-body model (PRBM) of compliant mechanisms. The legged SMA component can be seen as a compliant mechanism. The PRBM provides a simple method for analyzing compliant members that undergo nonlinear deflections by modeling their deflection using rigid-body components with equivalent force-deflection characteristics.

A diagram of the fixed-guided motion using a compliant beam and its corresponding PRBM is shown in Fig. 8a. One end of the legged component is fixed, and the other end has a deflection, which can be displaced in both the x and y directions with load. The mechanism can be accurately described by two rigid links connected at a pivot by a torsional spring along the beam. The torsional spring with nonlinear stiffness characteristics is placed at the pivot to represent the model stiffness and potential energy. It is located at a length of γl from the beam tip in its undeflected position. Here, γ is termed as the characteristic radius factor and l is the length of the beam. The characteristic radius, γl, is the radius of the circular deflection path traversed by the end of the pseudo-rigid-body link, and is also the length of the pseudo-rigid-body link. The movable link can rotate about the pivot by an angle Θ (Howell and Midha, 1995; Mattson *et al.*, 2004).

The pseudo-rigid-body angle, Θ, of which the rotation is restrained by a torsional spring of equivalent stiffness K_θ placed at the pivot. The coordinates of the end of a deflected beam may now be given by equations parameterized in terms of the pseudo-rigid-body angle Θ:

$$\frac{a}{l} = 1 - \gamma(1-\cos\Theta), \tag{9}$$

$$\frac{b}{l} = \gamma\sin\Theta, \tag{10}$$

where a and b are the horizontal and vertical coordinates of the deflected end, respectively.

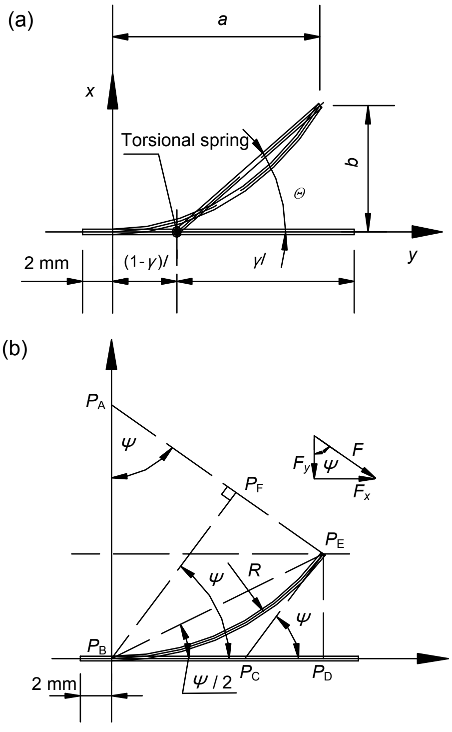

Fig. 8 Analysis of the legged component

(a) PRBM representation; (b) Force analysis. P_A, P_B, P_C, P_D, P_E, and P_F are the geometrical points of the beam, ψ is the slope of the end of the deflected beam, R is the deformed beam radius, and F is the force of the legged SMA structure exerted by the intestine

If the initial state of the beam is curved, then the characteristic radius factor is not the same. Define it as ρ, and define the initial beam curvature κ_0 as

$$\kappa_0=1/R_0, \tag{11}$$

where R_0 is the initial beam radius.

Taking the curvature into account, the length of the pseudo-rigid-body link (characteristic radius) is ρl, where ρ is a function of γ and the curvature, which can be calculated by

$$\rho=\left\{\left[\frac{a_0}{l}-(1-\gamma)\right]^2+\left(\frac{b_0}{l}\right)^2\right\}^{1/2}, \tag{12}$$

where a_0 and b_0 are the initial horizontal and vertical coordinates of the deflected end, respectively.

As the beam is initially curved, so the pseudo-rigid-body angle Θ has a non-zero initial value as

$$\Theta_0=\arctan\frac{b_0}{a_0-l(1-\gamma)}. \tag{13}$$

For the initial straight beam, $\rho=\gamma$, $a_0=1$, $b_0=0$, $\kappa_0=0$, and $\Theta_0=0$.

The torsion constant of the spring K is calculated as follows:

$$K=\rho K_\theta\frac{EI}{l}, \tag{14}$$

where I is the moment of the inertia, and K_θ can best be determined by a curve fit procedure.

From analysis of the legged component (Fig. 8b), it can be concluded:

$$F=\frac{F_x}{\sin\Psi}, \tag{15}$$

$$M_0=F\times P_BP_F=F\times P_AP_B\sin\psi=F_x\times P_AP_B=F_xR, \tag{16}$$

where M_0 means the torque generated at the fixed end.

The maximum stress occurs at the fixed end of the beam, and its value is as follows:

$$\sigma_{\max}=\frac{M_0c}{l}, \tag{17}$$

where c is the distance from the neutral axis to the outer fibers, and the pseudo-rigid-body angle is given by

$$M_0=K(\Theta-\Theta_0). \tag{18}$$

Considering the overall size requirements and the matching factor, the parameters of the legged SMA component is designed as: the thickness h=0.3 mm, the width w=1.6 mm, the total length l'=18 mm, the effective length l=16 mm, and the coordinates of the end of the deflected component at high temperature are a=13.73 mm, b=7 mm.

4.4 Prototype of the endoscopic robot

Fig. 9 shows the fabricated prototype of the endoscopic robot next to a coin. One can see the size of the endoscopic robot.

Fig. 9 Prototype of the endoscopic robot

As the motion of the small intestine is very complicated, it is a complex task to simulate intestinal movement. Thus, plastic pipes are used to simulate static gut, of which the diameters are between 20–15 mm close to that of the body's small intestine. During testing, the locomotive mechanism was effective in a plastic tube environment.

5 Summary and prospects

Endoscopic robots represent a significant technical breakthrough for the investigation of small intestine. Providing a capsule robot with active locomotion capabilities allows one to perform endoscopy in a totally controlled manner. This paper illustrates a legged locomotive mechanism with the SMA actuation based on the peristaltic principle. The capsule body is designed and fabricated with a hollow space for further integration with other components such as an RF module, a camera, and a battery. The locomotion mechanism and structure of this capsule robot are introduced, and then designs of the SMA spring and the legged component are described, as the core components of the locomotion system. We used the PRBM to analyze nonlinear and large deflections of the SMA legged component.

To evaluate the locomotive performance, several experiments in plastic tube tests were accomplished. In these experiments, the drive mechanism was effective in a plastic tube environment. The locomotion mechanism has the potential to be integrated into a wireless capsule endoscope for actuation.

Due to the complexity of this locomotion system, further research is needed, such as the simulation of the interaction between the legged microrobot and inner slippery surroundings of the GI tract. Our ongoing research aims to develop an autonomous microrobot in more depth firstly, and then to carry out tests in vivo. Finally, we will seek to reduce the overall size, and increase the traction ability of the endoscopic robot as much as possible to meet the actual needs of clinical applications.

References

Appleyard, M., Fireman, Z., Glukhovsky, A., Jacob, H., Shreiver, R., Kadirkamanathan, S., Lavy, A., Lewkowicz, S., Scapa, E., Shofti, R., *et al.*, 2000. A randomized trial comparing wireless capsule endoscopy with push enteroscopy for the detection of small-bowel lesions. *Gastroenterology*, **119**(6):1431-1438.

Cheung, E., Karagozler, M.E., Park, S., Kim, B., Sitti, M., 2005. A New Endoscopic Microcapsule Robot Using Beetle Inspired Microfibrillar Adhesives. IEEE/ASME International Conference on Advanced Intelligent Mechatronics, Monterey, CA, USA, p.551-557. [doi:10.1109/AIM.2005.1511040]

Gorini, S., Quirini, M., Menciassi, A., Pernorio, G., Stefanini, C., Dario, P., 2006. A Novel SMA-Based Actuator for a Legged Endoscopic Capsule. The First IEEE/RAS-EMBS International Conference on Biomedical Robotics and Biomechatronics, Pisa, Italy, p.443-449. [doi:10.1109/BIOROB.2006.1639128]

Howell, L.L., Midha, A., 1995. Parametric deflection approximations for end-loaded, large-deflection beams in compliant mechanisms. *Journal of Mechanical Design*, **117**(1):156-165.

Kim, B., Lee, S., Park, J.H., Park, J., 2004. Inchworm-Like Microrobot for Capsule Endoscope. IEEE International Conference on Robotics and Biomimetics, Shenyang, China, p.458-463. [doi:10.1109/ROBIO.2004.1521822]

Kim, B., Lee, S., Park, J.H., Park, J., 2005a. Design and fabrication of a locomotive mechanism for capsule-type endoscopes using shape memory alloys (SMAs). *IEEE/ASME Transactions on Mechatronics*, **10**(1):77-86. [doi:10.1109/TMECH.2004.842222]

Kim, B., Park, S., Jee, C.Y., Yoon, S., 2005b. An Earthworm-Like Locomotive Mechanism for Capsule Endoscopes. IEEE/RSJ International Conference on Intelligent Robots and Systems, Edmonton, AB, Canada, p.2997-3002. [doi:10.1109/IROS.2005.1545608]

Li, W.D., Guo, W., Li, M.T., Zhu, Y.H., 2006. Design and Test of a Capsule Type Endoscope Robot with Novel Locomation Principle. The 9th International Conference on Control, Automation, Robotics and Vision, Singapore, p.1-6. [doi:10.1109/ICARCV.2006.345240]

Mattson, C.A., Howell, L.L., Magleby, S.P., 2004. Development of commercially viable compliant mechanisms using the pseudo-rigid-body model: case studies of parallel mechanisms. *Journal of Intelligent Material Systems and Structures*, **15**:195-202.

Menciassi, A., Stefanini, C., Gorini, S., Pernorio, G., Kim, B., Park, J.O., Dario, P., 2004. Locomotion of a Legged Capsule in the Gastrointestinal Tract: Theoretical Study and Preliminary Technological Results. 26th Annual

International Conference of the IEEE Engineering in Medicine and Biology Society, San Francisco, CA, USA, p.2767-2770. [doi:10.1109/IEMBS.2004.1403791]

Moglia, A., Menciassi, A., Schurr, M.O., Dario, P., 2007. Wireless capsule endoscopy: from diagnostic devices to multipurpose robotic systems. *Biomed Microdevices*, **9**(2):235-243. [doi:10.1007/s10544-006-9025-3]

Moon, Y., Lee, J., Park, H., Lee, J., Ryu, J., Woo, S., Kim, M., Won, C., Kim, T., Cho, J., *et al.*, 2007. Fabrication of the wireless systems for controlling movements of the electrical stimulus capsule in the small intestines. *IEICE Transactions on Information and Systems*, **E90-D**(2): 586-593. [doi:10.1093/ietisy/e90-d.2.586]

Park, H., Park, S., Yoon, E., Kim, B., Park, J., Park, S., 2007. Paddling Based Microrobot for Capsule Endoscopes. IEEE International Conference on Robotics and Automation, Roma, Italy, p.3377-3382. [doi:10.1109/ROBOT.2007.363994]

Quirini, M., Scapellato, S., Valdastri, P., 2007. An Approach to Capsular Endoscopy with Active Motion. 29th Annual International Conference of the IEEE Engineering in Medicine and Biology Society, Lyon, France, p.2827-2830. [doi:10.1109/IEMBS.2007.4352917]

Rogers, C.L.C.A., 1997. Design of shape memory alloy springs with applications in vibration control. *Journal of Intelligent Material Systems and Structures*, **8**:314-322.

Sendoh, M., Ishiyama, K., Arai, K.I., 2003. Fabrication of magnetic actuator for use in a capsule endoscope. *IEEE Transactions on Magnetics*, **39**(5):3232-3234. [doi:10.1109/TMAG.2003.816731]

Yang, J., Wu, Y.H., 1993. Shape Memory Alloy and Its Applications. University of Science and Technology of China Press, Hefei, China, p.208-209 (in Chinese).

Zabulis, X., Sfakiotakis, M., Tsakiris, D.P., 2008. Effects of Vibratory Actuation on Endoscopic Capsule Vision. 30th Annual International Conference of the IEEE Engineering in Medicine and Biology Society, Vancouver, British Columbia, Canada, p.5901-5904. [doi:10.1109/IEMBS.2008.4650557]

Zhou, Y.S., Li, L.X., Zhao, D.F., 2001. New kind of microrobot. *Chinese Journal of Mechanical Engineering*, **37**(1):11-13 (in Chinese).